Inorg. Chem. **2009**, *48*, 3573−3580

Lanthanide Compounds with Fluorinated Aryloxide Ligands: Near-Infrared Emission from Nd, Tm, and Er

Kieran Norton,[†] G. A. Kumar,[‡] Jennifer L. Dilks,[†] Thomas J. Emge,[†] Richard E. Riman,*[,‡] Mikhail G. Brik,[§] and John G. Brennan*[,†]

Department of Chemistry and Chemical Biology, Rutgers, The State University of New Jersey, 610 Taylor Road, Piscataway New Jersey 08854-8087, Department of Materials Science & Engineering, The State University of New Jersey, 607 Taylor Road, Piscataway, New Jersey 08854-8065, and Institute of Physics, University of Tartu, Riia 142, Tartu 51014, Estonia

Received October 27, 2008

$Ln(OC_6F_5)_3$ form stable, isolable compounds with 1,2-dimethoxyethane (DME). Monomeric $(DME)_2Ln(OC_6F_5)_3$ (Ln = Nd, Er, Tm) adopt seven coordinate structures with two chelating DME and three terminal phenoxide ligands. Both $(py)_4Er(OC_6F_5)_3$ and $(THF)_3Yb(OC_6F_5)_3$ were also prepared and structurally characterized, with the latter being a *mer*-octahedral compound with bond lengths that are geometry dependent. Emission experiments on crystalline powders of the Nd(III), Tm(III), and Er(III) DME derivatives show that these compounds are highly emissive near-infrared sources.

Introduction

Fluorinated ligands impart unique chemical and physical properties to metal compounds,[1] including superior solubility/volatility properties, unusual crystal packing motifs, and the stabilization of elements in high oxidation states. In lanthanide chemistry, fluorination of organic ligands also leads to improved near-infrared (NIR) emission characteristics[2−4] that are potentially useful[5−9] in fields ranging from planar waveguide fiber amplification to infrared detection and imaging. Fluorination is useful in these applications as a way to reduce the number of C−H functional groups that vibrationally quench NIR emissions.[10]

Lanthanide compounds with a number of fluorinated ligand systems have been described, including acetates,[11] acetonylacetates,[12] *t*-butoxides,[13] amidos,[14] and thiolates.[2−4,15] Of these, only the fluorinated thiolate compounds have been probed photophysically, with stimulating results. Compounds of Er^{3+}, Nd^{3+}, and Tm^{3+} with SC_6F_5 ligands have been prepared in high yield, and in each case these compounds had NIR quantum efficiencies that were significantly greater than the efficiencies of previously reported molecular compounds. Both the absence of CH bonds in the anionic ligand and the low Ln−S phonon energies are thought to

* To whom correspondence should be addressed. E-mail: bren@rci.rutgers.edu (J.G.B.), riman@rci.rutgers.edu (R.E.R.).
[†] Department of Chemistry and Chemical Biology, Rutgers, The State University of New Jersey.
[‡] Department of Materials Science & Engineering, The State University of New Jersey.
[§] University of Tartu.

(1) (a) Chan, M. C. W. *Macromol. Chem. Phys.* **2007**, *208*, 1845. (b) Dias, H. V. R.; Fianchini, M. *Comments Inorg. Chem.* **2007**, *28*, 73. (c) Plenio, H. *ChemBioChem* **2004**, *5*, 650. (d) Witt, M.; Roesky, H. W. *Prog. Inorg. Chem.* **1992**, *40*, 353.
(2) Kumar, G. A.; Riman, R. E.; Diaz Torrez, L. A.; Garcia, O. B.; Banerjee, S.; Kornienko, A.; Brennan, J. G. *Chem. Mater.* **2005**, *17*, 5130.
(3) Banerjee, S.; Huebner, L.; Romanelli, M. D.; Kumar, G. A.; Riman, R. E.; Emge, T. J.; Brennan, J. G. *J. Am. Chem. Soc.* **2005**, *127*, 15900.
(4) Banerjee, S.; Kumar, G. A.; Emge, T. J.; Riman, R. E.; Brennan, J. G. *Chem. Mater.* **2008**, *20*, 4367.
(5) *Rare Earth Doped Fiber Lasers and Amplifiers*; Digonnet, M. J. F., Ed.; Marcel Dekker Inc: New York, 1993.
(6) Jha, A. *Proc. SPIE* **2006**, *6409*, 640918.
(7) Sokólska, I.; Ryba-Romanowski, W.; Golab, S.; Baba, M.; Wirkowiczc, M.; Ukasiewicz, T. *J. Phys. Chem. Solids* **2000**, *61*, 1573.
(8) de Camargo, A. S. S.; Nunes, L. A. O.; Botero, E. R.; Garcia, D.; Eiras, J. A. *Chem. Phys. Lett.* **2005**, *410*, 156.
(9) Becker, P. C.; Olsson, N. A.; Simpson, J. R. *Erbium doped fiber amplifiers- Fundamentals and Technology*; Academic Press: New York, 1999.
(10) (a) Riman, R. E.; Dejneka, M.; Ballato, J.; Snitzer, E. *Eur. J. Solid State Inorg. Chem.* **1995**, *32*, 873. (b) Ballato, J; Dejneka, M.; Snitzer, E.; Riman, R. E.; Zhou, W. *J. Mat. Res.* **1996**, *11*, 841. (c) Quochi, F.; Orru, R.; Cordella, F.; Mura, A.; Bongiovanni, G.; Artizzu, F.; Deplano, P.; Mercuri, M. L.; Pilia, L.; Serpe, A. *J. Appl. Phys.* **2006**, *99*, 053520/1–053520/4.
(11) (a) Fujihara, S.; Kato, T.; Kimura, T. *J. Sol-Gel Sci. Technol.* **2003**, *26*, 953. (b) Bombieri, G.; Benetollo, F.; Del Pra, A.; Oliveira, V. da Silva; Melo, D. M. A.; Zinner, L. B.; Vicentini, G. *J. Alloys Cmpd.* **2001**, *323*, 181. (c) Kang, S. J.; Jung, Y. S.; Sohn, Y. S. *Bull. Korean Chem. Soc.* **1997**, *18*, 75. (d) Bravo-Vasquez, J. P.; Ching, L. W. C.; Law, W. L.; Hill, R. H. *J. Photopolym. Sci. Technol.* **1998**, *11*, 589.

10.1021/ic8020639 CCC: $40.75
Published on Web 03/24/2009

minimize competitive vibrational relaxation pathways, and this in turn results in the formation of exceptionally emissive molecules.

The fluorinated phenoxide OC_6F_5 has been used frequently in main group[16] and transition metal[17] systems because it is a water stable anion,[18] it gives compounds that are soluble in organic solvents, and it is commercially available. Lanthanide complexes with OC_6F_5 anions have been described only for Eu(II), Eu(III), and a heterovalent Eu(II)/Eu(III) dimer, with structural characterization of the products revealing interesting π-π stacking interactions and dative Eu(II)-F bonds.[19] Application of the OC_6F_5 ligand to NIR emissive Ln is clearly warranted because the added air stability of this ligand relative to SC_6F_5 would be useful in materials fabrication, as long as higher energy Ln−O vibrations do not quench excited states. In this work, we extend the lanthanide chemistry of the OC_6F_5 ligand to the synthesis and characterization of thermally stable compounds of Nd, Er, and Tm, and investigate the NIR emission properties of powdered samples.

Experimental Section

General Methods. All syntheses were carried out under ultra pure nitrogen (WELCO CGI, Pine Brook, NJ), using conventional dry box or Schlenk techniques. Solvents (Fisher Scientific, Agawam, MA) were purified with a dual-column Solv-Tek solvent purification system (Solv-Tek Inc., Berryville, VA). Ln chips (Nd, Tm, Yb), Er powder, Hg (Strem Chemicals), PhSSPh (Acros), and HOC_6F_5 (Aldrich) were purchased and used as received. Melting points were recorded in sealed capillaries and are uncorrected. IR spectra were taken on a Thermo Nicolet Avatar 360 FTIR spectrometer, and recorded from 4000−600 cm^{-1} as a Nujol mull on NaCl plates. Elemental analyses were performed by Quantitative Technologies, Inc. (Whitehouse Station, NJ).

Synthesis of $(DME)_2Nd(OC_6F_5)_3$ (1). Nd (145 mg, 1.01 mmol), diphenyl disulfide (330 mg, 1.51 mmol), and Hg (20 mg, 0.1 mmol) were combined in DME (20 mL) and stirred for 48 h to give a light blue solution with blue precipitate. Pentafluorophenol (540 mg, 2.93 mmol) was added, and the solution was stirred for 5 days, resulting in a pale blue solution with a dark brown precipitate. The solution was filtered, concentrated to 5 mL, and layered with hexanes (10 mL) to give blue crystals (524 mg, 62%) that melted and turned purple at 104−107 °C. Anal. Calcd for $C_{26}H_{20}F_{15}O_7Nd$: C, 35.7; H, 2.29. Found: C, 35.7; H, 2.42. IR: 2960 (m), 2849 (w), 2668 (w), 2478 (w), 1650 (m), 1621 (w), 1509 (s), 1370 (w), 1309 (m), 1260 (m), 1172 (m), 1094 (s), 1018 (s), 858 (m), 799 (m), 721 (w), 635 (m) cm^{-1}.

Synthesis of $(DME)_2Er(OC_6F_5)_3$ (2). Er (165 mg, 0.988 mmol), diphenyl disulfide (326 mg, 1.50 mmol), and Hg (10 mg, 0.05 mmol) were combined in DME (20 mL) and stirred for 4 days to give a pink solution. Pentafluorophenol (550 mg, 2.99 mmol) was added, and the solution was stirred for 2 days to give a pink solution with a black precipitate. The solution was filtered, concentrated to 5 mL, and layered with hexanes (20 mL) to give pink crystals (529 mg, 60%) that melted at 122−129 °C. Anal. Calcd for $C_{26}H_{20}F_{15}O_7Er$: C, 34.8; H, 2.23. Found: C, 34.7; H, 2.42. IR: 2959 (m), 1652 (w), 1505 (s), 1475 (m), 1309 (w), 1246 (m), 1179 (m), 1098 (m), 1050 (s), 1022 (s), 988 (s), 873 (m), 862 (s), 800 (w), 636 (m) cm^{-1}.

Synthesis of $(DME)_2Tm(OC_6F_5)_3$ (3). Tm (167 mg, 0.998 mmol), diphenyl disulfide (328 mg, 1.50 mmol), and Hg (10 mg, 0.05 mmol) were combined in DME (20 mL) and stirred for 4 days to give a tan solution. Pentafluorophenol (550 mg, 2.99 mmol) was added, and the solution was stirred for 2 days resulting in a pale tan solution with a black precipitate. The solution was filtered, concentrated to 5 mL, and layered with hexanes (20 mL) to give colorless crystals (589 mg, 65%) that melted at 114−121 °C. Anal. Calcd for $C_{26}H_{20}F_{15}O_7Tm$: C, 34.7; H, 2.23. Found: C, 34.3; H, 2.15. IR: 2961 (m), 1650 (m), 1620 (w), 1503 (s), 1370 (w), 1309 (m), 1260 (m), 1177 (m), 1092 (s), 1048 (m), 1018 (s), 988 (s), 862 (m), 800 (m) cm^{-1}. Unit cell at 100 K from single crystal X-ray diffraction data: $P2_1/n$, $a = 10.3977(7)$ Å, $b = 12.7197(8)$ Å, $c = 23.4256(15)$ Å, $\beta = 96.483(1)$, $V = 3078.4(3)$ $Å^3$.

Synthesis of $(py)_4Er(OC_6F_5)_3$ (4). Er (165 mg, 0.988 mmol), diphenyl disulfide (325 mg, 1.49 mmol), and Hg (13 mg, 0.05 mmol) were combined in pyridine (30 mL), and the mixture was stirred for 5 days to give a pink solution. Pentafluorophenol (562 mg, 3.05 mmol) was added, and the solution was stirred for 7 days resulting in a pink solution with a black precipitate. The solution was filtered, concentrated to 5 mL, and layered with hexanes (5 mL) to give pink crystals (0.31 g, 30%) that melted at 127−130 °C. Anal. Calcd for $C_{38}H_{20}F_{15}N_4O_3Er$: C, 44.2; H, 1.95; N, 5.42. Found: C, 43.7; H, 2.00; N, 5.46. IR: 2962 (w), 1650 (m), 1602 (m), 1504 (s), 1444 (m), 1306 (m), 1260 (m), 1220 (w), 1172 (m), 1093 (w), 1068 (m), 1040 (w), 1016 (s), 988 (s), 799 (m), 752 (m), 701 (m), 625 (m) cm^{-1}.

Synthesis of $(THF)_3Yb(OC_6F_5)_3$ (5). Yb (0.193 g, 1.12 mmol), PhSSPh (0.370 g, 1.70 mmol), and Hg (0.016 g, 0.080 mmol) were

(12) (a) Malandrino, G.; Incontro, O.; Castelli, F.; Fragalà, I. L.; Benelli, C. *Chem. Mater.* **1996**, *8*, 1292. (b) Plakatouras, J. C.; Baxter, I.; Hursthouse, M. B.; Abdul Malik, K. M.; McAleese, J.; Drake, S. R. *J. Chem. Soc., Chem. Commun.* **1994**, 2455. (c) Rogachev, A. Y.; Minacheva, L. K.; Sergienko, V. S.; Malkerova, I. P.; Alikhanyan, A. S.; Stryapan, V. V.; Kuzmina, N. P *Polyhedron* **2005**, *24*, 723. (d) Condorelli, G. G.; Gennaro, S.; Fragalà, I. L. *Chem. Vapor Dep.* **2001**, *7*, 151. (e) Condorelli, G. G.; Gennaro, S.; Fragalà, I. L. *Chem. Vapor Dep.* **2000**, *6*, 185. (f) Condorelli, G. G.; Anastasi, G.; Fragalà, I. L. *Chem. Vapor Dep.* **2005**, *11*, 324. (g) Beach, D. B.; Collins, R. T.; Legoues, F. K.; Chu, J. O. *MRS Symp. Proc.* **1993**, *282*, 397. (h) Hirata, G. A.; McKittrick, J.; Yi, J.; Pattillo, S. G.; Salazar, K. V.; Trkula, M. *MRS Symp. Proc.* **1998**, *495*, 39.

(13) Bradley, D. C.; Chudzynska, H.; Hursthouse, M. B.; Motevalli, M.; Wu, R. *Polyhedron* **1994**, *13*, 1.

(14) Click, D. R.; Scott, B. L.; Watkin, J. G. *Chem. Commun.* **1999**, 633.

(15) (a) Melman, J.; Rhode, C.; Emge, T. J.; Brennan, J. G. *Inorg. Chem.* **2002**, *41*, 28. (b) Melman, J.; Emge, T. J.; Brennan, J. G. *Inorg. Chem.* **2001**, *40*, 1078.

(16) (a) Britovsek, G. J. P.; Ugolotti, J.; White, A. J. P. *Organometallics* **2005**, *24*, 1685. (b) Metz, M. V.; Sun, Y.; Stern, C. L.; Marks, T. J. *Organometallics* **2002**, *21*, 3691. (c) Whitmire, K. H.; Hoppe, S.; Sydora, O.; Jolas, J. L.; Jones, C. M. *Inorg. Chem.* **2000**, *39*, 85. (d) Jolas, J. L.; Hoppe, S.; Whitmire, K. H. *Inorg. Chem.* **1997**, *36*, 3335. (e) Jones, C. M.; Burkart, M. D.; Bachman, R. E.; Serra, D. L.; Hwu, S. J.; Whitmire, K. H. *Inorg. Chem.* **1993**, *32*, 5136.

(17) (a) Tremblay, T. L.; Ewart, S. W.; Sarsfield, M. J.; Baird, M. C. *Chem. Commun.* **1997**, 831. (b) Campbell, C.; Bott, S. G.; Larsen, R.; Van Der Sluys, W. G. *Inorg. Chem.* **1994**, *33*, 4950. (c) Amor, J. I.; Burton, N. C.; Cuenca, T.; Gomez-Sal, P.; Royo, P. *J. Organomet. Chem.* **1995**, *485*, 153. (d) Abbott, R. G.; Cotton, F. A.; Falvello, L. R. *Inorg. Chem.* **1990**, *29*, 514. (e) Dilworth, J. R.; Gibson, V. C.; Redshaw, C.; White, A. J. P.; Williams, D. J. *J. Chem. Soc., Dalton Trans.: Inorg. Chem.* **1999**, 2701. (f) Metz, M. V.; Sun, Y.; Stern, C. L.; Marks, T. J. *Organometallics* **2002**, *21*, 3691. (g) Ferreira Lima, G. L.; Araujo Melo, D. M.; Isolani, P. C.; Thompson, L. C.; Zinner, L. B.; Vicentini, G. *Anais Assoc. Brasil. Quim.* **2000**, *49*, 153. (h) Kim, M.; Zakharov, L. N.; Rheingold, A. L.; Doerrer, L. H. *Polyhedron* **2005**, *24*, 1803. (i) Buzzeo, M. C.; Iqbal, A. H.; Long, C. M.; Millar, D.; Patel, S.; Pellow, M. A.; Saddoughi, S. A.; Smenton, A. L.; Turner, J. F. C.; Wadhawan, J. D.; Compton, R. G.; Golen, J. A.; Rheingold, A. L.; Doerrer, L. H. *Inorg. Chem.* **2004**, *43*, 7709.

(18) (a) Ramirez, F.; Marecek, J. F. *Synthesis* **1979**, 71. (b) Kresge, A. J. *Chem. Soc. Rev.* **1973**, 475.

(19) Norton, K.; Emge, T. J.; Brennan, J. G. *Inorg. Chem.* **2007**, *46*, 4060.

Table 1. Summary of Crystallographic Details for **1**, **2**, **4**, and **5**[a]

compound	**1**	**2**	**4**	**5**
empirical formula	$C_{26}H_{20}F_{15}NdO_7$	$C_{26}H_{20}ErF_{15}O_7$	$C_{38}H_{20}ErF_{15}N_4O_3$	$C_{30}H_{24}F_{15}O_6Yb$
fw	873.66	896.68	1032.84	938.53
space group	$P2_12_12_1$	$P2_1/n$	$P2_1/c$	$C2/c$
a (Å)	10.3931(2)	10.3977(7)	11.9793(6)	11.423(1)
b (Å)	13.1499(3)	12.7197(7)	15.5793(8)	17.907(2)
c (Å)	44.970(1)	23.426(2)	20.030(1)	16.435(1)
β (deg)	90.00	96.483(1)	90.471(1)	92.225(1)
V (Å^3)	6146.0(2)	3078.4(3)	3738.1(3)	3359.2(5)
Z	8	4	4	4
D(calcd) (g/cm^{-3})	1.888	1.935	1.835	1.856
abs coeff (mm^{-1})	1.824	2.860	2.365	2.909
$R(F)^b$ [$I > 2\ \sigma(I)$]	0.0353	0.0319	0.0201	0.0258
$R_w(F^2)^c$ [$I > 2\ \sigma(I)$]	0.0765	0.0779	0.0475	0.0640

[a] All data were collected at 100(2)°K using Mo Kα radiation ($\lambda = 0.71073$ Å). [b] $R(F) = \sum||F_o| - |F_c||/\sum|F_o|$. [c] $R_w(F^2) = \{\sum[w(F_o^2 - F_c^2)^2]/\sum w(F_o^2)^2\}^{1/2}$. Additional crystallographic details are given in the Supporting Information.

added to THF (20 mL), and the mixture was stirred for 6 days at room temperature to give an opaque dark red solution. C_6F_5OH (0.635 g, 3.45 mmol) was added, and the reaction was stirred for 8 days and then filtered to separate trace gray precipitate. The colorless solution was concentrated to about 5 mL and layered with hexanes (~10 mL) to give translucent colorless crystals that turn white at 179 °C and melt/turn yellow at 195−199 °C. Anal. Calcd for $C_{30}H_{24}YbF_{15}O_6$: C, 38.4; H, 2.58. Found: C, 37.9; H, 2.38. The UV−vis (THF) spectrum contained one peak at 313 nm ($\varepsilon = 1 \times 10^2$ L mol^{-1} cm^{-1}). IR: 2963 (w), 2283 (w), 1655 (w), 1509 (s), 1384 (s), 1260 (m), 1173 (w), 1019 (m), 992 (m), 800 (m) cm^{-1}. Unlike the analogous fluorinated thiolate derivative that reacts instantly with water to form a lightly colored precipitate, this compound does not appear to react with water at room temperature.

X-ray Structure Determination. Data for compounds **1**, **2**, **4**, and **5** were collected on a Bruker Smart APEX CCD diffractometer with graphite monochromatized Mo Kα radiation ($\lambda =$ 0.71073Å) at 100 K. Crystals were immersed in Paratone oil and examined at low temperatures. The data were corrected for Lorenz effects and polarization, and absorption, the latter by a multiscan (SADABS)[20] method. The structures were solved by direct methods (SHELXS86).[21] All non-hydrogen atoms were refined (SHELXL97)[22] based upon F_{obs}^2. All hydrogen atom coordinates were calculated with idealized geometries (SHELXL97). Scattering factors (f_o, f', f'') are as described in SHELXL97. Crystallographic data and final R indices for **1**, **2**, **4**, and **5** are given in Table 1. POV-ray diagrams[23] for **1**, **2**, **4**, and **5** are shown in Figures 1−4 respectively. Complete crystallographic details are given in the Supporting Information.

Spectroscopy. Absorption measurements were carried out with crystalline powder using an integrating sphere of a double beam spectrophotometer (Perkin-Elmer Lambda 9, Wellesley, MA).The emission spectra of the powdered samples were recorded by exciting the sample with the 800 nm band of a Ti-Sapphire laser (for Nd and Tm) and with a 980 nm diode laser for the Er sample. The emission from the sample was focused onto a 0.55 m monochromator (Jobin Yvon, Triax 550, Edison, NJ) and detected by a thermoelectrically cooled InGaAs detector. The signal was intensified with a lock-in amplifier (SR 850 DSP, Stanford Research System, Sunnyvale, CA) and processed with a computer controlled by SynerJY commercial software. To measure the decay time, the laser beam was modulated by a chopper, and the signal was collected on a digital oscilloscope (TDS 220, 200 MHz, Tektronix, Beavetron, OR). The emission data analysis follows our earlier work.[24]

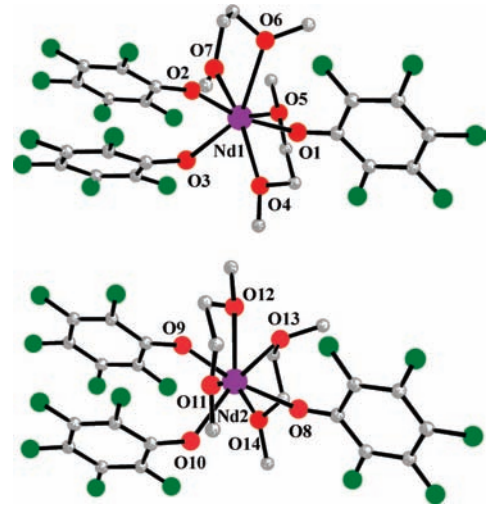

Figure 1. POVRAY diagram of the two crystallographically independent molecules within the unit cell of $(DME)_2Nd(OC_6F_5)_3$, with green F, white C, and the hydrogen atoms removed for clarity. Significant distances (Å) and angles (deg): Nd(1)−O(1), 2.238(2); Nd(1)−O(2), 2.272(2); Nd(1)−O(3), 2.287(2); Nd(1)−O(7), 2.511(2); Nd(1)−O(4), 2.512(2); Nd(1)−O(6), 2.544(2); Nd(1)−O(5), 2.546(2); C(1)−O(1)−Nd(1), 166.9(2); C(7)−O(2)−Nd(1), 152.7(2); C(13)−O(3)−Nd(1), 129.4(2); Nd(2)−O(8), 2.241(2); Nd(2)−O(10), 2.271(2); Nd(2)−O(9), 2.273(2); Nd(2)−O(11), 2.488(2); Nd(2)−O(12), 2.532(2); Nd(2)−O(13), 2.539(2); Nd(2)−O(14), 2.547(2); C(27)−O(8)−Nd(2), 163.2(2); C(33)−O(9)−Nd(2), 152.1(2); C(39)−O(10)−Nd(2), 129.5(2).

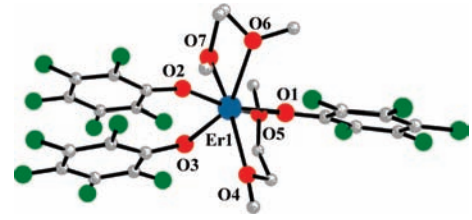

Figure 2. POVRAY diagram of $(DME)_2Er(OC_6F_5)_3$, with green fluorine, white carbon, and the hydrogen atoms removed for clarity.Significant distances (Å) and angles (deg): Er(1)−O(1), 2.150(2); Er(1)−O(2), 2.180(2); Er(1)−O(3), 2.183(2); Er(1)−O(4), 2.390(2); Er(1)−O(6), 2.413(2); Er(1)−O(5), 2.423(2); Er(1)−O(7), 2.426(2); C(1)−O(1)−Er(1), 164.7(2); C(7)−O(2)−Er(1), 149.2(2); C(13)−O(3)−Er(1), 132.7(2).

(20) *SADABS, Bruker Nonius area detector scaling and absorption correction*, v2.05; Bruker-AXS Inc.: Madison, WI, 2003.
(21) Sheldrick, G. M. *SHELXS86, Program for the Solution of Crystal Structures*; University of Göttingen: Göttingen, Germany, 1986.
(22) Sheldrick, G. M. *SHELXL97, Program for Crystal Structure Refinement*; University of Göttingen: Göttingen, Germany, 1997.
(23) *Persistence of Vision Raytracer*, Version 3.6; Persistence of Vision Pty. Ltd.: 2004; [Computer software retrieved from http://www.povray.org/download/].

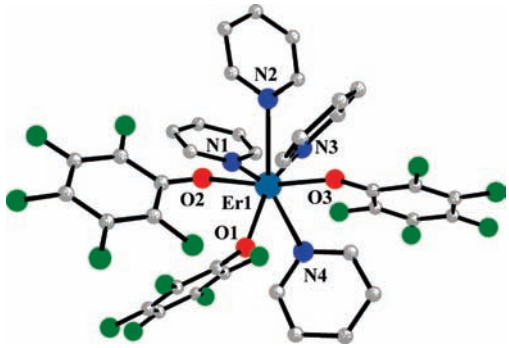

Figure 3. POVRAY diagram of $(py)_4Er(OC_6F_5)_3$, with green fluorine, white carbon, and the hydrogen atoms removed for clarity.Significant distances (Å) and angles (deg): Er(1)−O(3), 2.164(1); Er(1)−O(2), 2.182(1); Er(1)−O(1), 2.186(1); Er(1)−N(1), 2.4919(13); Er(1)−N(4), 2.5175(14); Er(1)−N(2), 2.5446(13); Er(1)−N(3), 2.5464(13); C(13)−O(3)−Er(1), 168.8(1); C(7)−O(2)−Er(1), 160.0(1); C(1)−O(1)−Er(1), 149.1(1).

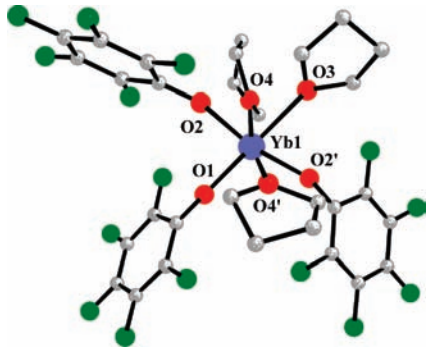

Figure 4. POVRAY diagram of $(THF)_3Yb(OC_6F_5)_3$, with green fluorine, white carbon, and the hydrogen atoms removed for clarity.Significant distances (Å) and angles (deg): Yb(1)−O(1), 2.084(2); Yb(1)−O(2), 2.111(2); Yb(1)−O(2)′, 2.111(2); Yb(1)−O(4)′, 2.296(2); Yb(1)−O(4), 2.296(2); Yb(1)−O(3),2.332(2);O(1)−Yb(1)−O(2),95.76(4);O(1)−Yb(1)−O(2)′, 95.76(4); O(2)−Yb(1)−O(2)′, 168.48(9); O(1)−Yb(1)−O(4)′, 97.35(4); O(2)−Yb(1)−O(4)′,88.07(7);O(2)′−Yb(1)−O(4)′,90.46(7);O(1)−Yb(1)−O(4), 97.35(4); O(2)−Yb(1)−O(4), 90.46(7); O(2)′−Yb(1)−O(4), 88.07(7); O(4)′−Yb(1)−O(4), 165.30(9); O(1)−Yb(1)−O(3), 180.0; O(2)−Yb(1)−O(3), 84.24(4); O(2)′−Yb(1)−O(3), 84.24(4); O(4)′−Yb(1)−O(3), 82.65(4); O(4)−Yb(1)−O(3), 82.65(4); C(1)−O(1)−Yb(1), 180.0; C(5)−O(2)−Yb(1), 162.3(1).

Results

Fluorinated phenoxides of the NIR emissive lanthanides are prepared at room temperature in high yields by metathetical reactions of in situ prepared $Ln(SPh)_3$ with HOC_6F_5. Thermally stable DME derivatives $(DME)_2Ln(OC_6F_5)_3$ were isolated for Ln = Nd(**1**), Er(**2**), and Tm(**3**) and characterized by low temperature single crystal X-ray diffraction. All three compounds are isomorphous, with the Nd compound crystallographically distinct from the isostructural Er and Tm compounds. Figures 1 and 2 contain POVRAY diagrams for the Nd and Er/Tm compounds, respectively, with significant bond geometries given in the figure captions. In both **1** and **2**, the seven coordinate Ln bond to three terminal aryloxides and four neutral oxygen donors from two chelating DME ligands. There are no significant Ln−F dative interactions.

THF and pyridine derivatives were also prepared in an attempt to isolate octahedral compounds that might show anomalous bond length distributions. From pyridine, $(py)_4Er(OC_6F_5)_3$ (**4**) was isolated. Figure 3 contains a POVRAY diagram of **4**, with significant distances and angles given in the figure caption. This seven coordinate molecule is best described as a pentagonal bipyramid, and as found in the DME compounds, there are only terminal phenoxide ligands with no significant Ln−F interactions. The THF compound $(THF)_3Yb(OC_6F_5)_3$ was also isolated, and low temperature diffraction experiments showed that the molecule adopts a meridional conformation. Figure 4 contains a POVRAY diagram of **5**, with significant distances and angles given in the figure caption. In this molecule, there are Ln−O(C_6F_5) bonds trans to both phenolate and neutral THF donors, and there appears to be a slight but statistically significant dependence of Ln−O bond length upon the identity of the trans ligands. The two crystallographically related Ln−O(C_6F_5) bonds that are trans to phenolates (Ln−O(2) = 2.111(2) Å) are longer by 0.027 Å than is the Ln−O phenlolate bond trans to THF (2.084(2) Å). The same trend is noted in the bonds to THF, where the Ln−O(C_4H_8) bond trans to the phenolate 2.332(2) Å is 0.036 Å longer than the Ln−O bonds trans to THF (2.296(2) Å).

The room temperature absorption spectra for the NIR active Nd, Er, and Tm compounds (**1**, **2**, and **3**, respectively) are shown in Figures 5a, 6a, and 7a, respectively. The absorption bands for **1**, **2**, and **3** are identified using the standard notations summarized in Tables 2, 3, and 4, respectively. All absorption profiles were numerically integrated to evaluate the experimental oscillator strengths. The measured oscillator strengths were fitted with theoretical oscillator strength values to obtain the three phenomenologi-

Table 2. Experimentally Observed Band Positions, Their Integrated Absorbance, Experimental and Calculated Oscillator Strengths for $(DME)_2Nd(OC_6F_5)_3$

transitions	energy (cm^{-1})	$\int\alpha(\lambda)\,d\lambda$ (10^{-7})	$f_{(exp)}$ (10^{-6})	$^af_{(cal)}$ (10^{-6})
$^2P_{3/2}$	25189	2.14	0.119	excluded
$^2D_{5/2}$ + $^2P_{3/2}$	24450	1.14	0.059	0.0030
$^2P_{1/2}$	23095	1.09	0.051	0.0720
$^4G_{11/2}$ + $^2G_{9/2}$ + $^2K_{15/2}$	21322	0.98	0.039	0.0470
$^4G_{7/2}$ + $^4G_{9/2}$	19531	1.83	0.061	0.3236
$^2K_{13/2}$ + $^2G_{7/2}$	17889	18.4	0.516	0.3264
$^4G_{5/2}$ + $^2H_{11/2}$	16367	58.2	1.363	1.3605
$^4F_{7/2}$ + $^4S_{3/2}$	13831	1.82	0.031	0.0509
$^4F_{5/2}$ + $^2H_{9/2}$	12937	20.2	0.295	0.2556
$^4F_{3/2}$	11848	22.1	0.272	0.2134

^{a} $\Omega_2 = 0.388 \times 10^{-20}$ cm^2, $\Omega_4 = 0.539 \times 10^{-20}$ cm^2, and $\Omega_6 = 0.327 \times 10^{-22}$ cm^2; RMS =1.37 $\times$ 10^{-7}.

Table 3. Experimentally Observed Band Positions, Their Integrated Absorbance, Experimental and Calculated Oscillator Strengths for $(DME)_2Er(OC_6F_5)_3$

band	energy (cm^{-1})	$\int\alpha(\lambda)\,d\lambda$ (10^{-7}cm)	$f_{(exp)}$ (10^{-6})	$^af_{(cal)}$ (10^{-6})
$^4G_{11/2}$	24631	2.91	6.82	7.13
$^4F_{3/2}$	23810	12.0	26.2	excluded
$^4F_{5/2}$ + $^4F_{3/2}$	22321	1.36	2.62	1.58
$^4F_{7/2}$	20202	1.44	2.27	3.20
$^2H_{11/2}$	18832	3.27	4.49	3.93
$^4S_{3/2}$	17123	1.05	1.19	0.76
$^4F_{9/2}$	14409	4.38	3.52	3.23
$^4I_{9/2}$	11905	1.01	0.554	0.328

^{a} $\Omega_2 = 1.54 \times 10^{-20}$ cm^2, $\Omega_4 = 2.29 \times 10^{-20}$ cm^2 and $\Omega_6 = 2.05 \times 10^{-20}$ cm^2; RMS = 0.81 $\times 10^{-6}$; Fluorescence decay time =1 ms, Radiative decay time = 6.17 ms, QE = 16%.

(24) Kumar, G. A.; Riman, R. E.; Torres, L. A. D.; Banerjee, S.; Romanelli, M. D.; Emge, T. J.; Brennan, J. G *Chem. Mater.* **2007**, *19*, 2937.

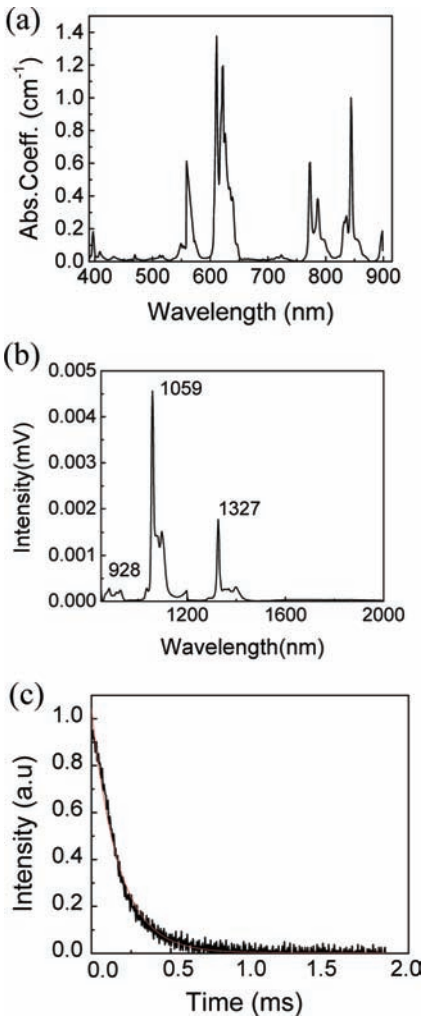

Figure 5. Absorption (a), emission (b), and fluorescence decay (c) curves of $(DME)_2Nd(OC_6F_5)_3$.

cal intensity parameters. The parameters obtained for **1** are $\Omega_2 = 0.388 \times 10^{-20}$ cm^2, $\Omega_4 = 0.539 \times 10^{-20}$ cm^2, $\Omega_6 = 0.327 \times 10^{-22}$ cm^2, for **2** are $\Omega_2 = 15.5 \times 10^{-20}$ cm^2, $\Omega_4 = 3.28 \times 10^{-20}$ cm^2, $\Omega_6 = 4.62 \times 10^{-20}$ cm^2, and for **3** are $\Omega_2 = 1.54 \times 10^{-20}$ cm^2, $\Omega_4 = 2.29 \times 10^{-20}$ cm^2, and $\Omega_6 = 2.05 \times 10^{-20}$ cm^2 with rms values of 0.137×10^{-6} (Nd) and 2.04×10^{-6} (Tm) and 0.81×10^{-6} (Er) between the experimental and theoretical oscillator strengths.

NIR Emission spectra of the three compounds are shown in Figures 5b (Nd), 6b (Er), and 7b (Tm). All three compounds show emission with characteristic band positions, that is, Nd^{3+} at 928 ($^4F_{3/2} \rightarrow {}^4I_{9/2}$), 1059 ($^4F_{3/2} \rightarrow {}^4I_{11/2}$), and 1327 nm ($^4F_{3/2} \rightarrow {}^4I_{13/2}$); Tm^{3+} at 1458 ($^3H_4 \rightarrow {}^3H_5$), 1759 ($^3F_4 \rightarrow {}^3H_6$), and Er^{3+} at 1550 nm ($^4I_{13/2} \rightarrow {}^4I_{15/2}$). Relative intensities are not comparable because of differences in sample concentrations.

To measure the quantum efficiency of the main emission transition the effective fluorescence decay times (τ_{eff}) for **1**−**3** were extracted from the measured decay curves shown in Figures 5c, 6c, and 7c, respectively. Decay curves were fitted with the exponential curve fit to yield decay times of 170 μs for the 1059 nm emission from **1**, 1 ms for the 1552 nm emission band of **2**, and 145 and 127 μs, respectively for the 1458 and 1759 nm bands from **3**. The effective

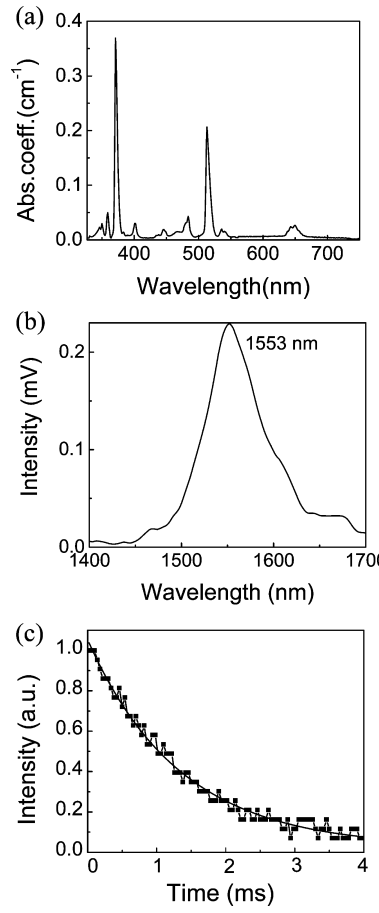

Figure 6. Absorption (a), emission (b), and fluorescence decay (c) curves of $(DME)_2Er(OC_6F_5)_3$.

experimental decay time (τ_{eff}), together with the calculated Judd−Ofelt[25] radiative decay time of 8.6 ms for **1**, results in a calculated quantum efficiency of nearly 2% for **1**. For **2** an efficiency of 16% was obtained (1552 nm with a radiative decay time of 6.16 ms), and for **3** the efficiencies of the two bands are 1.9% (1458 nm) and 4.5% (1759 nm).

Assuming a Gaussian line shape the stimulated emission cross sections of the emission transitions can be evaluated using the Füchtbauer−Ladenburg equation[26]

$$\sigma_{em} = \frac{\lambda^4 A}{8\pi c n^2 \Delta\lambda_{eff}}$$

where $\Delta\lambda_{eff}$ is the effective line-width of the emission band obtained by integrating over the entire emission band and dividing by the peak fluorescence intensity. According to the above equation the calculated emission cross sections are 0.061×10^{-20} cm^2 (928 nm), 0.082×10^{-20} cm^2 (1059 nm) for **1**, (1552 nm) 0.54×10^{-20}cm^2 and 0.9×10^{-20} cm^2 (1458 nm) for **2**, and 6.5×10^{-20}cm^2 (1759 nm) for **3**. Tables 5 and 6 summarize the radiative spectral properties of **1** and **3**. The emission cross sections are greater than the values reported for either crystalline or amorphous inorganic materi-

(25) (a) Judd, B. R. *Phys. Rev. B* **1962**, *127*, 750. (b) Ofelt, G. S. *J. Chem. Phys.* **1962**, *37*, 511.
(26) Kaminskii, A. A. *Laser Crystals: Their Physics and Properties*; Springer Verlag: New York, 1981.

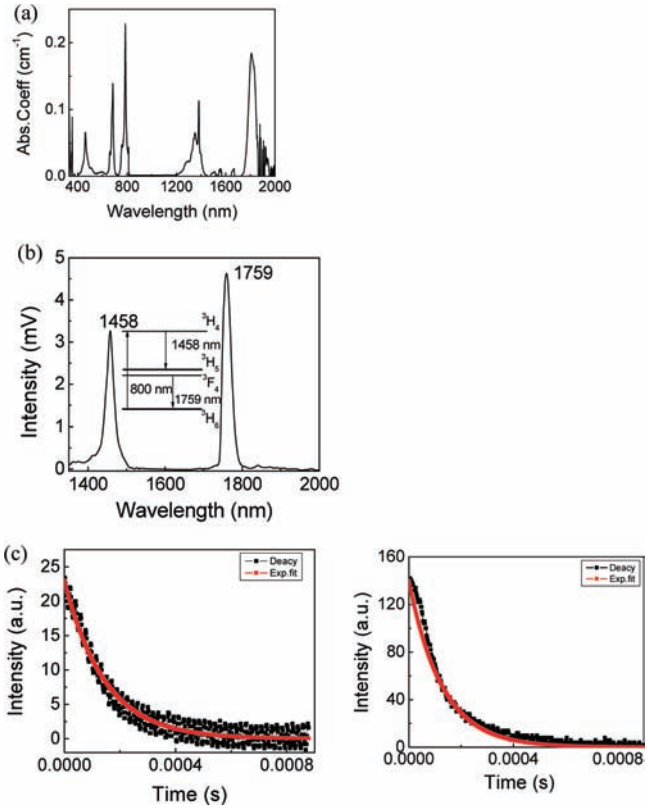

Figure 7. Absorption (a), emission (b), and fluorescence decay (c) curves of $(DME)_2Tm(OC_6F_5)_3$.

Table 4. Experimentally Observed Band Positions, Their Integrated Absorbance, Experimental and Calculated Oscillator Strengths for $(DME)_2Tm(OC_6F_5)_3$

transitions	energy (cm^{-1})	$\int\alpha(\lambda)\,d\lambda$ (10^{-7})	$f_{(exp)}$ (10^{-6})	$^af_{(cal)}$ (10^{-6})
$^1D_2$	28169	1.10	5.60	4.63
$^1G_4$	21598	5.41	16.1	excluded
$^3F_2+^3F_3$	14619	6.60	9.02	9.97
$^3H_4$	12722	10.9	11.3	9.57
$^3H_5$	7235	14.5	4.85	4.34
$^3F_4$	5530	28.1	5.49	7.32

$^a\,\Omega_2 = 15.5 \times 10^{-20}$ cm^2, $\Omega_4 = 3.28 \times 10^{-20}$ cm^2 and $\Omega_6 = 4.62 \times 10^{-20}$ cm^2; RMS $= 2.04 \times 10^{-6}$.

als.[27] The higher stimulated emission cross section results from the lower effective bandwidths, compared to amorphous materials that have a range of 60−80 nm. The narrow bandwidth and high stimulated emission cross sections facilitates the application of these materials as high gain optical amplifiers.

Discussion

Stable adducts of the trivalent fluorinated phenoxides $Ln(OC_6F_5)_3$ can be isolated in high yields as either DME, THF, or pyridine complexes. The metals react incompletely with HOC_6F_5, but reactions can be driven to completion by first solubilizing Ln using the in situ preparation of $Ln(SPh)_3$, followed by a proton transfer reaction with HOC_6F_5 to give $Ln(OC_6F_5)_3$ [reactions 1 and 2]. Structural characterization of the DME adducts

$$Ln + \frac{3}{2}PhSSPh \rightarrow \text{“}Ln(SPh)_3\text{”} \quad (1)$$

$$\text{“}Ln(SPh)_3\text{”} + HOC_6F_5 \rightarrow Ln(OC_6F_5)_3 + 3HSPh \quad (2)$$

revealed essentially the same seven coordinate structures as found in the fluorinated thiolates, with chelating DME ligands and terminal aryloxides. The pyridine compound **4** similarly contained four neutral donor atoms saturating the Er(III) coordination sphere with only terminal phenoxide ligands being observed.

An octahedral derivative was isolated only when the sterically more demanding THF ligand was coupled with the smallest of the Ln to generate *mer*-octahedral **5**. This geometry was targeted to examine whether bond lengths in these fluorinated phenoxides would exhibit any directional dependence. The possibility that lanthanide compounds might exhibit structural trans-influence was noted at least as early as 1995 by Deacon,[28] who compared a pair of isomorphous aryloxide compounds with different neutral donor ligands, and by our laboratory,[29] in the description of *mer*-$(py)_3Yb(SPh)_3$. At that time, these observations conflicted with the standard view of structure and bonding in lanthanide systems,[30] namely that bond lengths could be predicted and rationalized by summing the ionic radii of the lanthanide ion and the donor ligand,[31] with the metal ionic radius dependent only on charge and coordination number. In subsequent years, *fac*-octahedral halide coordination compounds,[32] chalcogenolate complexes,[33] and chalcogenido based cluster compounds with octahedral Ln geometries[34] have been described. In every case, an analysis of the Ln-anion bond length distribution revealed that bonds trans to anions are consistently longer than bonds trans to neutral donors. At first glance, compound **5** also exhibits this directional bonding effect, with the Ln−O(C_6F_5) bonds trans to phenoxides being significantly longer than the Ln−O bond trans to the neutral THF donor.

Unfortunately, the tendency of these phenoxides to engage in π-π stacking interactions makes it more difficult to unambiguously interpret Ln−O distances. In all of the seven coordinate structures **1**, **2**, and **4**, there are distributions of

(27) (a) Yang, Z.; Luo, L.; Chen, W. *J. Appl. Phys.* **2006**, *99*, 076107. (b) Truong, V. G.; Jurdyc, A. M.; Jacquier, B.; Ham, B. S.; Quang, A. Q. L.; Leperson, J.; Nazabal, V.; Adam, J. L. *J. Opt. Soc. Am. B.* **2006**, *23*, 2588. (c) CanoTorres, J. M.; Serrano, M. D.; Zaldo, C.; Rico, M.; Mateos, X.; Liu, J.; Griebner, U.; Petrov, V.; Valle, F. J.; Galan, M.; Viera, G. *J. Opt. Soc. Am. B* **2006**, *23*, 2594. (d) Balda, R.; Lacha, L. M.; Fernandez, J. M.; Fernandez-Navarro, J. M. *Proc. SPIE* **2005**, *55*, 5723.

(28) Deacon, G. B.; Feng, T.; Skelton, B. W.; White, A. H. *Aust. J. Chem.* **1995**, *48*, 741.

(29) Lee, J.; Brewer, M.; Berardini, M.; Brennan, J. *Inorg. Chem.* **1995**, *34*, 3215.

(30) Raymond, K. N.; Eigenbrot, C. W. *Acc. Chem. Res.* **1980**, *13*, 276.

(31) Shannon, R. D. *Acta Crystallogr. A* **1976**, *32*, 751.

(32) (a) Deacon, G. B.; Feng, T.; Junk, P. C.; Skelton, B. W.; Sobolev, A. N.; White, A. H. *Aust. J. Chem.* **1998**, *51*, 75. (b) Deacon, G. B.; Feng, T.; Junk, P. C.; Meyer, G.; Scott, N. M.; Skelton, B. W.; White, A. H. *Aust. J. Chem.* **2000**, *53*, 853.

(33) (a) Aspinall, H. C.; Cunningham, S. A.; Maestro, P.; Macaudiere, P. *Inorg. Chem.* **1998**, *37*, 5396. (b) Mashima, K.; Nakayama, Y.; Fukumoto, H.; Kanehisa, N.; Kai, Y.; Nakamura, A. *J. Chem. Soc., Chem. Commun.* **1994**, 2523.

(34) (a) Freedman, D.; Melman, J. H.; Emge, T. J.; Brennan, J. G. *Inorg. Chem.* **1998**, *37*, 4162. (b) Kornienko, A.; Emge, T.; Hall, G.; Brennan, J. G. *Inorg. Chem.* **2002**, *41*, 121.

Table 5. Radiative Properties of $(DME)_2Nd(OC_6F_5)_3$

transition from $^4F_{3/2}$ to	wavelength (nm)	S_{ed} (10^{-20}) (cm^2)	A (s^{-1})	$\Delta\lambda_{eff}$ (nm)	τ_{rad} (ms)	τ_{fl} (ms)	σ_e (10^{-20}) (cm^2)
$^4I_{15/2}$	1843	0.000092	0.00775		8.6		
$^4I_{13/2}$	1327	0.0007	0.15718	26.2	8.6	0.17	0.00092
$^4I_{11/2}$	[a]1059	0.078	81.71141	27.2	8.6		0.082
$^4I_{9/2}$	928	0.124	34.49011	51	8.6		0.061

[a] $\eta = 2\%$

Table 6. Radiative Properties of $(DME)_2Tm(OC_6F_5)_3$

transition	wavelength (nm)	$\Delta\lambda_{eff}$ (nm)	$\sigma_e(10^{-20})$ (cm^2)	τ_{rad} (μs)	τ_{fl} (μs)	η (%)
$^3H_4 \rightarrow {}^3F_4$	1458	34	0.9	7518	145	1.9
$^3F_4 \rightarrow {}^3H_6$	1759	27	6.5	2776	127	4.5

Ln−O(C_6F_5) distances with a range of separations (ca. 0.03 Å) that are identical to the difference between the long and short Ln−O bonds in octahedral structure **5**. In each of the seven coordinate structures, the two phenoxides with the longer Ln−O bond lengths are the ligands that are interacting through π-π stacking interactions.

This is not to suggest that a covalent interaction would represent anything more than a small contribution to complex stability, because the remaining structural features can all be discussed in electrostatic terms. For example, while it has been noted in the past that there appears to be no significant correlation of bond length with Ln−O−C angle, in compounds **1**−**5** the phenoxide with the longest Ln−O bond length usually has the most obtuse Ln−O−C angle (which range from 129−180° in all compounds). The trend is present in the structures of **1**, **2**, and **5**, with the exception being the structure of compound **4**, for which two of the phenoxides have statistically indistinguishable Ln−O bond lengths but dramatically different Ln−O−C angles. An electrostatic model to explain this behavior has been proposed[35] and is consistent with the observations here.

Similarly, electrostatic effects also presumably account for the fact that all of the Ln(III)−OR are terminally bound, even when crystallized from solvents as weakly basic as DME. Alkoxide compounds are relatively insoluble materials because the concentration of electron density on the small, highly electronegative oxide donor atom increases the tendency for these ligands to bridge metal centers by displacing neutral donors from Ln coordination spheres. However, fluorination of the ring reduces electron density at the phenolate oxygen, rendering it less able to displace neutral donors from Ln coordination spheres.

Finally, the consistent absence of Ln−F dative interactions for the trivalent compounds contrasts with the frequent observation of these "bonds" in analogous fluorinated thiolates. This difference can be rationalized by noting that the more electronegative oxygen ligand has less electron density delocalized throughout the arene, rendering the fluorides less electron rich. An alternative explanation for the absence of dative Ln−F bonds would be that the electrostatic opening of these Ln−O−C angles relative to Ln−S−C results in a displacement of the entire fluorinated ring away from the Ln coordination sphere. The fact that dative Ln−F bonds were noted in divalent Eu−OC_6F_5 structures (including a heterovalent compound for which Eu(II)−F but not Eu(III) interactions were observed) can be explained by noting that electrostatic bond strengths depend strongly on metal oxidation state, and so for Ln(II) compounds the entropy gain associated with displacing a neutral Lewis base ligand with a chelating Ln−F interaction is more likely to compensate for the relative weakness of the Ln−F bond.

The three NIR emissive Ln ions investigated in this work show different emission properties and efficiencies that can be interpreted in terms of their structure and coordination environments. A comparison of these $(DME)_2Ln(OC_6F_5)_3$ compounds with their thiolate analogues $(DME)_2Ln(SC_6F_5)_3$ offers a unique opportunity to evaluate how S replacing O influences molecular emission properties. The NIR quantum efficiencies of $(DME)_2Nd(SC_6F_5)_3$ (9%), $(DME)_2Tm(SC_6F_5)_3$ (2% for $^3H_4 \rightarrow {}^3F_4$ and 0.1% for $^3F_4 \rightarrow {}^3H_6$), and $(DME)_2Er(SC_6F_5)_3$ (75%) were found to be considerably greater than previous literature values for more traditional Nd(III),[36] Tm(III),[37] and Er(III)[38] coordination compounds. The lower quantum efficiencies of **1** (2%), **2** (19%), and **3** (1.9% and 4.5%) relative to their fluorinated thiolate counterparts can be understood by noting that non-radiative losses due to the relatively high frequency vibronic coupling of the coordinated alkoxide decreases the relative intensity of the phenolate emission. An additional potential contributor to non-radiative quenching is de-excitation to the triplet states of the arene ligands that are close to the excitation levels, but unfortunately a quantitative assessment of this process for both SR and OR compounds, as well as alternative processes, namely, excitation migration or cross relaxation, and so forth, can only be obtained from detailed energy

(35) Russo, M. R.; Kaltsoyannis, N.; Sella, A. *Chem. Commun.* **2002**, 2458.

(36) (a) Hasegawa, Y.; Ohkubo, T.; Gogabe, K.; Kawamura, Y.; Wada, Y.; Nakashima, N.; Yanagida, S. *Angew. Chem., Int. Ed.* **2000**, *39*, 357. (b) Klink, S. I.; Hebbink, G. A.; Grave, L.; van Veggel, F. C. J. M.; Reinhoudt, D. N.; Slooff, L. H.; Polman, A.; Hofstraat, J. W. *J. Appl. Phys.* **1999**, *86*, 1181. (c) Hebbink, G. A.; van Veggel, F. C. J. M.; Reinhoudt, D. N. *Eur. J. Org. Chem.* **2001**, 4101. (d) Hasegawa, Y.; Murakoshi, K.; Wada, Y.; Kim, J. H.; Nakashima, N.; Yamanaka, T.; Yanagida, S. *Chem. Phys. Lett.* **1996**, *248*, 8. (e) Wada, Y.; Okubo, T.; Ryo, M.; Nakazawa, T.; Hasegawa, Y.; Yanagida, S. *J. Am. Chem. Soc.* **2000**, *122*, 8583.

(37) (a) Alexey, V. T.; Carpenter, A. V.; Gorokhovsky, A. A.; Alfano, R. R.; Chu, T. Y.; Okamoto, Y. *Proc. SPIE* **1998**, *165*, 3468. (b) Kaizaki, S.; Shirotani, D.; Tsukahara, Y.; Nakata, H. *Eur. J. Inorg. Chem.* **2005**, *1*, 3503. (c) Zang, F. X.; Hong, Z. R.; Li, W. L.; Li, M. T.; Sun, X. Y. *Appl. Phys. Lett.* **2004**, *84*, 2679.

(38) (a) Hebbink, G. A.; Reinboudt, D. N.; van Veggel, F. C. J. M. *Eur. J. Org. Chem.* **2001**, 4101. (b) Wolbers, M. P. O.; van Veggel, F. C. J. M.; Snellink-Ruel, B. H. M.; Hofstraat, J. W.; Geurts, F. A. J.; Reinhoudt, D. N. *J. Am. Chem. Soc.* **1997**, *119*, 138. (c) Wolbers, M. P. O.; van Veggel, F. C. J. M.; Peters, F. G. A.; E.van Beelen, E. S.; Hofstraat, J. W.; Geurts, F. A. J.; Reinhoudt, D. N. *Chem.—Eur. J.* **1998**, *4*, 772. (d) Hasegawa, Y.; Okhubo, T.; Sogabe, K.; Kawamura, Y.; Wada, Y.; Nakashima, N.; Yanagida, S. *Angew. Chem., Int. Ed.* **2000**, *39*, 357.

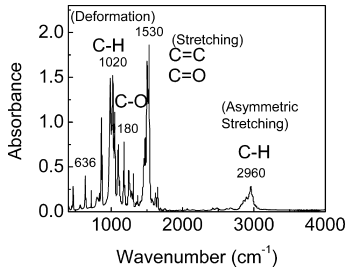

Figure 8. FTIR spectrum of $(DME)_2Nd(OC_6F_5)_3$; the spectra of the analogous Er and Tm compounds are indistinguishable.

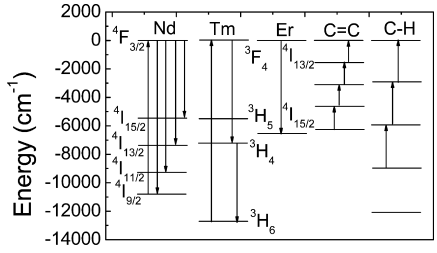

Figure 9. Energy level diagram for comparing the relative energy levels of the three emissive Ln ions and the fluorescence quenching C−H and C−C overtones.

transfer calculations, which are currently in progress.

The other structural aspect that impacts upon emission intensity is the presence of ligands with C−H and C═C bonds, because of the well documented quenching through coupling to ligand C═C and C−H vibrations. The FTIR spectrum of **1** given in Figure 8 shows the presence of several such vibronic groups in these compounds, particularly C═C stretching at 1530 cm^{-1}, C−H deformation at 1020 cm^{-1}, and C−H asymmetric stretching at 2960 cm^{-1}. The vibronic energy transfer coupling can be interpreted with the help of the energy level diagram shown in Figure 9. From the figure it can be seen that the fourth order C═C vibration is almost in resonance with the Er^{3+} emission with a difference of energy of 278 cm^{-1}. Similarly the second order vibration of C−H is almost in resonance with Er^{3+} emission with an energy difference of 603 cm^{-1}. Because of these vibronic couplings, the C═C and C−H functional groups are likely to be significant quenchers of Er emission in complex **2**. Similarly, in the Nd^{3+} complex **1** the third order C−H vibrational band is in resonance with the 1060 nm emission with an energy difference of 316 cm^{-1} and is likely to be the major cause of the reduced efficiency of 1060 nm emission in complex **1**. The two NIR emission bands of the Tm^{3+} compound **3** are least affected by these vibronic couplings.

With direct coordination of Ln to heavier sulfur atoms, the coupling between the energy levels is less efficient and the Franck−Condon factor for the relaxation process is reduced, effectively increasing the lifetime of the thiolate compounds relative to the phenoxides. Unfortunately, in terms of device fabrication, the thiolate compounds suffer from a tendency to react with water. For example, $(py)_3Yb(SC_6F_5)_3$ reacts instantly with water in pyridine; the red color that has been assigned as a S-to-Yb charge transfer absorption[39] disappears, and a light yellow solid precipitates. Identical experiments with the phenoxide derivatives do not give hydrolysis products. The phenoxides, while not as emissive as their thiolate counterparts, are considerably more NIR emissive than most (if not all) prior molecular NIR sources. If quantum efficiencies can be increased further by eliminating the CH functional groups on the DME ligands (i.e., displacement by donor functional groups of a polymer), then Ln complexes with these relatively air stable OC_6F_5 anions will be attractive candidates for polymer waveguide amplifiers.

Conclusion

Trivalent lanthanide complexes with OC_6F_5 ligands can be prepared in high yield and isolated as DME, THF, or pyridine adducts. The DME and py compounds adopt seven coordinate pentagonal bipyramidal structures, while the THF derivative is a *mer*-octahedral structure with inequivalent Ln−O bond lengths. The DME compounds are all NIR emissive, although not as bright as their thiolate counterparts, but any decrease in emission intensity is partially compensated for by the greater air stability of the phenoxide anion.

Acknowledgment. This material is based upon work supported by the National Science Foundation under CHE-0747165. R.E.R. and G.A.K. acknowledge ONR-DARPA-ONR under Grant 428833.

Supporting Information Available: Crystal data and structure refinement, atomic coordinated and equivalent isotropic displacement parameters, bond lengths and angles, anisotropic displacement parameters, and torsion angles for **1**−**3** and **5**. This material is available free of charge via the Internet at http://pubs.acs.org.

IC8020639

(39) Lee, J.; Freedman, D.; Melman, J. H.; Brewer, M.; Sun, L.; Emge, T. J.; Long, F. H.; Brennan, J. G. *Inorg. Chem.* **1998**, *37*, 2512.